Journal of Physics: Conference Series **420** (2013) 012120 doi:10.1088/1742-6596/420/1/012120

Study of the fusion reaction ^{12}C + ^{12}C at low beam energy

C.L. Jiang[1], M. Albers[1], S. Almaraz-Calderon[1], M. Alcorta[1], B.B. Back[1], P. Bertone[1], B. Bucher[2], P. Collon[2], S. Courtin[3], C.M. Deibel[1], B. DiGiovine[1], H. Esbensen[1], X. Fang[2], J. Greene[1], F. Haas[3], D.J. Henderson[1], R.V.F. Janssens[1], T. Lauritsen[1], A. Lefebvre-Schuhl[4], C.J. Lister[1], S.T. Marley[1], R. Pardo[1], M. Paul[5], K.E. Rehm[1], D. Seweryniak[1], X.D. Tang[2], C. Ugalde[1], S. Zhu[1]

[1]Physics Division, Argonne National Laboratory, Argonne, IL 60439, USA,
[2]University of Notre Dame, Notre Dame, IN 46556, USA,
[3]Universite de Strabourg, F-67037 Strasbourg Cedex 2, France,
[4]Universite Paris Sud, F-91405 Orsay, France,
[5]Hebrew University,Jerusalem 90914, Israel

E-mail: jiang@phy.anl.gov

Abstract. In this article we discuss two aspects related to the ^{12}C + ^{12}C fusion reaction at low energies for carbon burning in supermassive stars. First we present plausible arguments for the notion that the observed resonance structures at the lowest measured energies arise from the relatively large spacing and narrow width of ^{24}Mg compound levels at the corresponding excitation energy region. We thus point out that the Incoming Wave Boundary Condition is inappropriate for calculating the fusion cross section under these situations. Secondly, we report on a particle-γ coincidence technique that has been used for the first time to measure the fusion cross section in the system ^{12}C + ^{12}C at low beam energies. Based on these results, it should be possible to measure this important fusion cross section down to the 10 pb level within a reasonable length of time.

1. Introduction

Fusion reactions between ^{12}C nuclei are important in the history of stellar evolution, especially in the scenarios of highly developed stars, where these reactions are important routes for the production of heavier elements [1, 2, 3, 4]. Because of their importance in nuclear astrophysics, many measurements of these fusion reactions have been performed in the past. Although these processes occur at high temperatures in explosive scenarios, the Gamow energies are still very low resulting in extremely small cross sections at the interesting excitation energies. In order to obtain the astrophysical reaction rates one has, therefore, to rely on the theoretical calculations or phenomenological extrapolations. All these expectations depend on the understanding of the reaction mechanism involved.

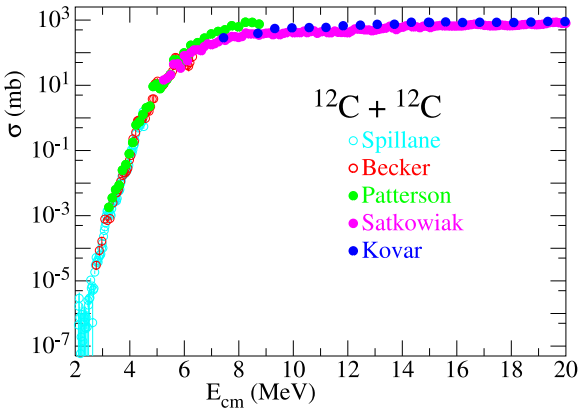

Figure 1. The excitation function of fusion reaction ^{12}C + ^{12}C.

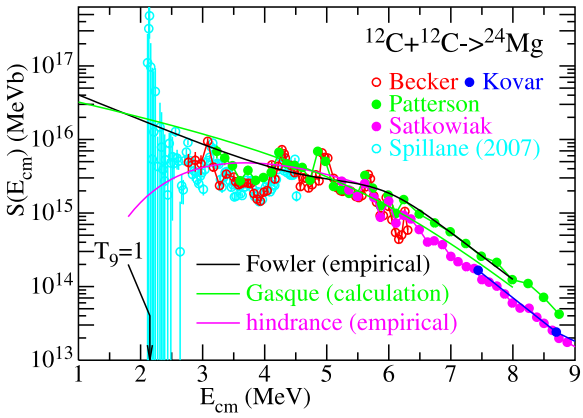

Figure 2. The S factor of ^{12}C + ^{12}C fusion as a function of center-of mass energy E_{cm}.

The excitation function of ^{12}C + ^{12}C fusion is presented in Fig. 1. There have been many measurements published in the literature, of which only some are shown [5, 6, 7, 8, 9]. These measurements cover more than 10 orders of magnitude. In order to compensate for the strong Coulomb effect, the S factor is used ($S(E) = \sigma E e^{2\pi\eta}$, where η is the Summerfeld parameter) which is presented in Fig. 2. Heavy-ion fusion hindrance has been observed at very low energies in recent years [10, 11], and it was explained as being due to the saturation properties of nuclear matter [12]. The expected extrapolations for the S factor of ^{12}C + ^{12}C depend very much on the various recipes. Calculations with the barrier penetration model (green) [4] and empirical extrapolations with hindrance (magenta) [10] are two examples, which give opposite trends with decreasing energies.

2. The fusion reaction ^{12}C + ^{12}C at low energies

It is well known that there are "resonance structures" in the excitation functions of ^{12}C + ^{12}C, ^{12}C + ^{16}O and ^{16}C + ^{16}O. Among them ^{12}C + ^{12}C shows the most pronounced peaks followed by ^{12}C + ^{16}O and ^{16}O + ^{16}O. Resonances (isolated or overlapping) have been well studied in fusion reactions induced by light ions. On the contrary, the excitation functions of heavy-ion fusion reactions are generally smooth in heavy systems. This is consistent with the Incoming Wave Boundary Condition (IWBC) which assumes that there is full absorption of incoming waves reaching a certain point inside the barrier and the compound levels are available at the actual energy, spin and parity. This condition is only satisfied if the level density of the compound nucleus is high, and the level widths are broader than the level distances.

It was already pointed out by Almqvist *et al.* in their pioneering paper [13] that the resonance structure occurring in ^{12}C + ^{12}C may be due to the low excitation energy of the compound nucleus ^{24}Mg. Erb *et al.* (from the same collaboration, [14]) however, later came to the conclusion that apart from the narrow resonances, the average energy dependence of the ^{12}C + ^{12}C can be described adequately by a compound-nucleus reaction, using the IWBC calculations of Christensen *et al.*, [15].

Aguilera *et al.* in their measurements [16] suggested to reproduce the excitation function of ^{12}C + ^{12}C by the formula:

$$\sigma_{fus}(E) = \sigma_{bkg}(E) + \sigma_{BW}(E). \quad (1)$$

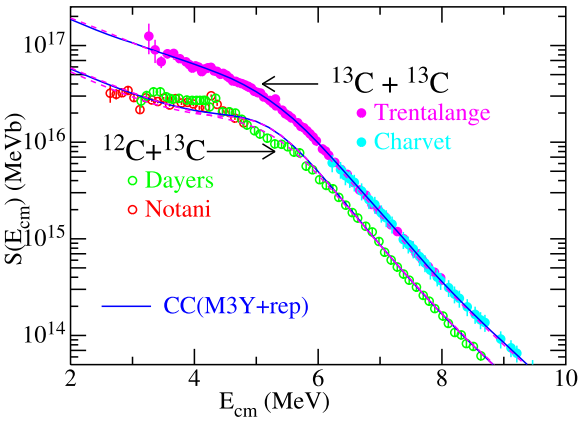

Figure 3. $S(E_{cm})$ for the fusion reactions ^{12}C + ^{13}C [19, 20] and ^{13}C + ^{13}C [21, 22]. The solid curves are CC(M3Y+rep) calculations [18].

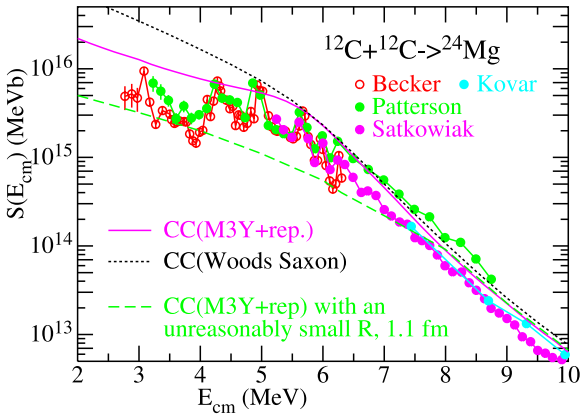

Figure 4. $S(E_{cm})$ for the fusion reaction ^{12}C + ^{12}C. The magenta curve is a calculation of CC(M3Y+rep.) [18].

Here $\sigma_{BW}(E)$ is the contribution of resonances and σ_{bkg} is the 'background' component, calculated with the one-dimensional barrier penetration model (BPM) by using the Krappe-Nix-Sierk potential [17]. Essentially, they explicitly assumed that for the barrier penetration model the absorption is complete, and the level density of the compound nucleus is high enough that the IWBC is valid. This separation into 'resonance' and 'background' contributions, however, is somewhat artificial and unproven.

Recently, detailed Coupled-Channels calculations CC(M3Y+rep) were performed for three isotope systems of carbon collisions, ^{13}C + ^{13}C, ^{12}C + ^{13}C and ^{12}C + ^{12}C by Esbensen *et al.,* [18] in order to ascertain whether it is possible to reproduce the experimental data of all three systems with the aid of the M3Y+rep potential, which was developed in the study of the heavy-ion fusion hindrance [12]. The main points in this CC(M3Y+rep) calculations were : 1) The IWBC assumption has been used, which means that the absorption is complete after the penetration through the barrier. 2) The potential used is a shallow one, due to the contribution of the repulsive core. That is, the calculation already takes care of the hindrance property, and is much lower than the one from CC(Woods Saxon) at low energies. 3) The couplings used are rather complete, including the mutual excitations and the transfer reactions. 4) In the calculation, parameters for the nucleus ^{13}C and ^{12}C were calibrated to reproduce the experimental data of ^{13}C + ^{13}C and ^{12}C + ^{13}C (see Fig. 3). 5) In the calculations for fusion of ^{12}C + ^{12}C, no free parameters were used, since all parameters have been fixed in the calculations for other two systems.

Since in the CC(M3Y+rep) calculations mentioned above, the potential, the couplings *etc.*, have been adjusted to the data for ^{12}C + ^{13}C and ^{13}C + ^{13}C, the calculations for ^{12}C + ^{12}C should predict the right flux in the entrance channel. The results (see magenta curve in Fig. 4) however, overestimate the experimental cross sections at the lowest energies, and reproduce them only at the resonance peaks. In order to reproduce the cross sections at the valleys the interaction radius R in the CC(M3Y+rep) calculations should be decreased to an unreasonable, extraordinary small value, 1.1 fm, which is included in Fig. 4 as dashed-green curve.

This is an indication that at most the absorption of the penetrated flux is incomplete. We interpret this result as that, the level density of the compound nucleus is not being high enough

for the IWBC to be applicable. Only at the molecular resonances, is the level density of the compound nucleus high enough to guarantee the complete absorption.

The reason that this effect is especially pronounced in the ^{12}C + ^{12}C fusion is that the fusion Q value for ^{12}C + ^{12}C $\rightarrow$ ^{24}Mg reactions is extraordinary low ($Q = 13.934$ MeV). In addition, the nucleus ^{24}Mg is even-even, which results in a lower level density due to the higher pair energy. Also, due to the fact that there are identical particles in the entrance channel, negative parity states can not be involved in the fusion reactions. It was already suggested by Vandenbosch [23] that, "if there are not overlapping compound states of the relevant angular momentum ($\Gamma_J/D_J < 1$), fusion will not complete successfully". Here Γ_J and D_J are the level width and the level spacing of compound states with angular momentum J. He applied this idea for high angular momentum parts of the ^{12}C + ^{12}C fusion reaction at higher excitation energies. In the following we will discuss the effect of paucity of levels for the reaction ^{12}C + ^{12}C at low energies. In CC calculations, the excitation function for ^{12}C + ^{12}C at low energies is expressed as

$$\sigma(E) = \Sigma\sigma_J(E), \quad J = 0, 2, 4, 6, 8, \tag{2}$$

where J is the total angular momentum. If the level density is not high enough, a factor $P_J(E)$ should be added,

$$\sigma(E) = \Sigma[\sigma_J(E)P_J(E)], \quad J = 0, 2, 4, 6, 8. \tag{3}$$

The factor P_J describes the effect of non-overlapping compound levels. Clearly for strongly overlapping levels, *i.e.* $\Gamma/D >> 1$, this factor should be unity, and in the non-overlapping region one may expect it to approach the value Γ/D. Thus the first approximation for P_J, fulfilling these requirements is

$$P_J(E) = \begin{cases} 1 & \text{for } \Gamma_J(E)/D_J(E) \geq 1 \\ \Gamma_J(E)/D_J(E) & \text{for } \Gamma_J(E)/D_J(E) < 1. \end{cases} \tag{4}$$

Iljinov *et al.,* [24] have analysed the level densities of compound nuclei at energies appropriate to this paper, by providing phenomenological fits to the experimental data [25].The experimental total level densities for ^{24}Mg, ^{25}Mg and ^{32}S nuclei are reproduced in Fig. 5. Iljinov listed also the fitted level-density parameter a of the well-known level-density formula (for example Eq. (2) of Ref. [24]) for each data point. The dependence of the level density, $\rho(U)$ on energy was obtained by fitting the parameters $a(E)$ with a polynomial:

$$a(E) = C_1 + C_2U + C_3U^2, \tag{5}$$

where U is the excitation energy and C_1, C_2 and C_3 are adjusted parameters. The $\rho(U)$ were obtained with the $a(E)$ and the formulas from Ref. [24] and results are shown in Fig. 5 as solid curves. These curves describe the experimental level densities quite well. Though the experimental data do not reach high excitation energies, they do cover the energy region important for this paper. Light-blue arrows touch the curves in Fig. 5 represent the fusion Q values of these three systems. It is important to note that, the level density for the nucleus ^{25}Mg is higher than the one for ^{24}Mg by a factor of more than 50 at zero incident energies.

The density of level for a specific spin and parity, is given by the relation

$$\rho(U, J^\pi) = \frac{(2J+1)e^{-(J+1/2)^2/2\sigma^2}}{4\sigma^3\sqrt{2\pi}}\rho(U), \tag{6}$$

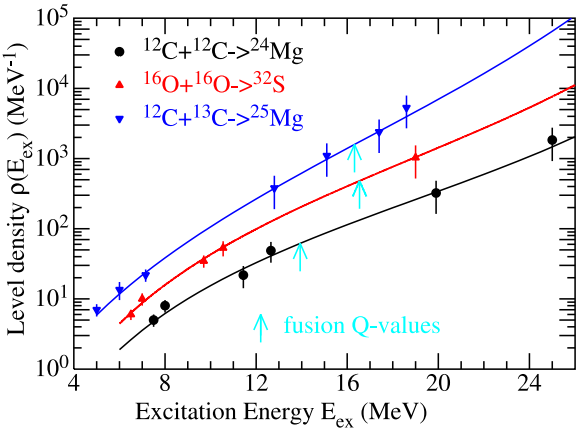

Figure 5. Level densities for the nuclei ^{24}Mg, ^{25}Mg and ^{32}S. The solid curves are obtained from fits to the data. For ^{24}Mg, ^{25}Mg and ^{32}S, the parameters obtained are C_1 = 4.914, 4.637, 5.678, C_2 = −0.1953, −0.1067, −0.2048 and C_3 = 0.004575, 0.003699, 0.004796, respectively.

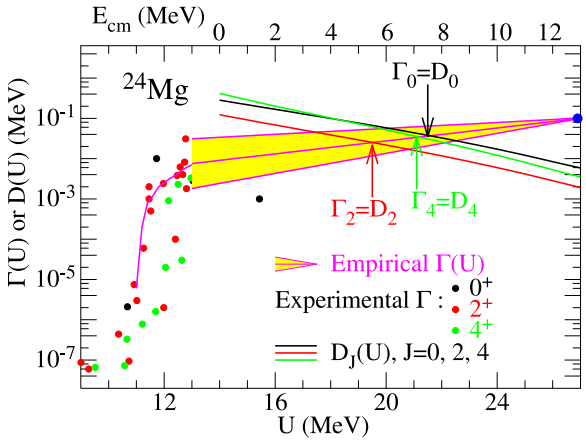

Figure 6. Widths $\Gamma(U)$ and level spacings $D_J(U)$ in ^{24}Mg as functions of the excitation energy U for levels of spin, $J = 0, 2$ and 4. The corresponding center-of-mass energy, E_{cm} for ^{12}C+^{12}C fusion is given on the top. The energy at which $\Gamma_J = D_J$ is indicated by arrows for each spin value.

where $\sigma^2 = 0.088aTA^{2/3}$ is the spin cutoff parameter, $T = \sqrt{U/a}$ is the nuclear temperature, A the mass of the compound nucleus, and $\rho(U)$ is the total level density

$$\rho(U) = \frac{\sqrt{\pi}}{12}\frac{\exp 2\sqrt{aU}}{a^{1/4}U^{5/4}}. \tag{7}$$

The other characteristic of the compound levels that comes into play is their width $\Gamma_J(U)$, which we assume to correspond to the total escape width into the various open decay channels. There are no detailed comparisons between direct experimental measurements and calculations of $\Gamma_J(U)$ for lighter systems in the literature. However, experimental values of level widths for ^{24}Mg in the BNL table are shown in Fig. 6 for J =0, 2 and 4 [26]. The spread of experimental $\Gamma_J(U)$, *e.g.* for $J = 2$ is more than an order of magnitude at around $U = 13$ MeV, just below the threshold energy. The only other, more or less certain value for $\Gamma(U)$ at higher energy is around 0.1 MeV, as used by Vandenbosch from Ericson fluctuations studies [23]. Combining all these values we construct an approximate, J-independent $\Gamma(U)$ band (representing by magenta curves) shown in Fig. 6.

Also shown in Fig. 6 are the average level spacings D_J obtained from Eq.(6) for $J = 0, 2$ and 4. The energy at which the average level width equals the average level spacing (for the mid-magenta curve) changes with spin J as indicated by arrows in Fig. 6. These energies are 7.6, 5.8 and 7.0 MeV for $J = 0$, 2 and 4, respectively. Around and below these energies, it is expected that the fusion cross section, for a specific entrance $L = J$ value is reduced relative to the one obtained from the Coupled-Channels IWBC calculation. At higher energies, cross sections for higher angular momenta contribute successively, and this energy region was discussed by Vandenbosch [23]. The energy value for $J = 0$ denoted as E_g, will be used as a reference energy in the following discussion. The $\Gamma_J(E), D_J(E) = 1/\rho_J(E)$ curves from Fig. 6 are used in Eqs. (3, 4) to calculate the corrected fusion cross sections and the results are shown in Fig. 7 by the blue curves. Here, the partial cross sections $\sigma_J(E)$ obtained by Coupled-Channels calculations with the M3Y+rep potential (magenta curve shown in Fig. 7) are used.

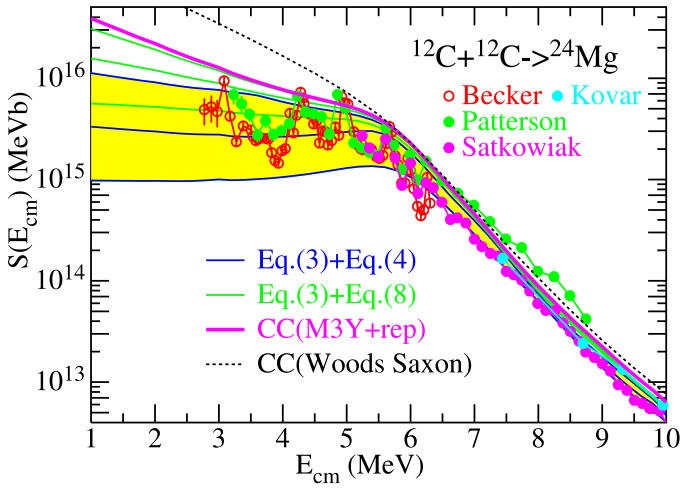

Figure 7. Comparison of different calculations with the experimental S factor of ^{11}C+^{12}C fusion. The magenta curve is from a CC(M3Y+rep) calculation without the corrections for the paucity for level-density [18]. The band formed by blue curves is obtained with the correction of Eq. (4).

It is not our attempt to quantitatively reproduce the experimental data at the valleys but rather to show the reduced effect due to the paucity of level density. The calculations do show, however, that in the fusion of ^{12}C + ^{12}C, the level density of the compound nucleus around 7 MeV, is not high enough, and, thus, absorption may be not complete for the penetrating flux. We also want to note that, at slightly higher energies, where $\Gamma_J(E)/D_J(E) > 1$, absorption could also be incomplete due to the effect of statistical fluctuation in the level distributions.

There were other choices for the correction factor $P_J(E)$ other than Eq. (4). Vandenbosch proposed that, the absorption probability is 0.5 when $\Gamma_J/D_J = 1$, and he adopted, somewhat arbitrarity, a Fermi function $P_l(E) = 1/(1 + \exp{(E_l^c - E)/b})$ to describe the absorption correction for different angular momentum l [23]. However, in an earlier publication [27] Moldauer analyzed the issue of non-overlapping resonances within the context of R-matrix theory and obtained an average transmission coefficient of $T = 1 - \exp(-2\pi\overline{\Gamma}/D)$. For comparison, we also use this expression, namely,

$$P_J(E) = 1 - \exp{(-2\pi\overline{\Gamma}_J/D_J)}, \tag{8}$$

to replace the Eq. (4). The results are shown in Fig. 7 by the green curves. From Eq. (4) and Eq. (8), it can be realized easily that, at very low energies (low values of Γ_J/D_J), the corrected cross sections based on Eq. (8) are about a factor of 6 higher than the one based on Eq. (4). Right now we don't want to make a judgement about the validity of these correction factors, instead we leave this question open to the future.

The center-of-mass energy E_g, at which $\Gamma_0(E)/D_0(E) = 1$ for the system ^{12}C + ^{12}C is listed in the first line of Table I. Together with the fusion Q value one obtains the corresponding excitation energy in the compound nucleus, E_{ex}^g. In that excitation energy region, the level-density effect is important. Similar estimations are performed for some neighboring systems, ^{12}O + ^{16}O, ^{16}C + ^{16}O, ^{12}C + ^{13}O, ^{13}C + ^{13}C, ^{10}B + ^{12}C and ^{10}B + ^{10}B. From Table I it can be seen that the paucity of compound levels would appear in other systems at lower excitation energies. For

Table 1. Center of mass energies, E_g at which the calculated Γ_0/D_0 is ~ 1. Q and E^g_{ex} are the fusion Q values and the corresponding excitation energies.

System	E_g(MeV)	Q(MeV)	E^g_{ex}(MeV)
$^{12}C + ^{12}C$	7.5	13.934	21.4
$^{12}C + ^{16}O$	2.5	16.765	19.3
$^{16}O + ^{16}O$	0.6	16.542	17.2
$^{12}C + ^{13}C$	-0.9	16.318	15.4
$^{13}C + ^{13}C$	-6.0	22.465	16.5
$^{10}B + ^{12}C$	-1.7	17.233	16.5
$^{10}B + ^{10}B$	-10.0	31.143	21.1

the systems $^{12}C + ^{16}O$ and $^{16}O + ^{16}O$, non-pronounced resonance phenomena have already been observed as expected from Table I. For the other four systems, the corresponding energies, E_g are negative. No resonance structure is expected for these systems, which is in perfect agreement with the experimental observations.

Another interesting observation can be made from Fig. 7. With decreasing bombarding energy the average level widths relative to the level spacing also decrease. As a result the oscillatory structures observed for $^{12}C + ^{12}C$ become deeper. This behavior, the suppression of the S factor at low energies will result in lower reaction rates than estimated by the recipes used in the previous astrophysical calculations.

To summarize this part: a new understanding of the resonance structures in the fusion of $^{12}C + ^{12}C$ at low excitation energies has been suggested. Due to the paucity of compound levels in ^{24}Mg, absorption is not complete in the energy region where resonances occur, especially at the valleys of the excitation function. The shortage of levels is remedied at the resonance peaks due to the presence of the molecular resonances. Thus the Ingoing Wave Boundary Conditions is not always satisfied in lighter heavy-ion fusion reactions. It would be very interesting to extend the measurements for fusion of $^{12}C + ^{12}C$, $^{12}C + ^{16}C$ and $^{16}C + ^{16}C$ toward lower energies in the future. A possible technique will be discussed in the following sections.

3. The particle-γ coincidence technique for measurements of $^{12}C + ^{12}C$ fusion cross sections

From a comparison of experimental excitation functions of the fusion reaction $^{12}C + ^{12}C$ one observes large deviations among the various experimental data. Recently there has been some controversy about the possible existence of a new strong resonance at $E_{cm} = 2.14$ MeV. This resonance, with cross sections reaching 1.5 nb, was first observed by studying the γ rays from the ^{23}Na evaporation residues [9]. However, a subsequent measurement using the charged-particle technique by the same collaboration gave a preliminary cross section of only about 25 pb [29]. This discrepancy underlines the importance of measuring the fusion cross sections in $^{12}C + ^{12}C$ down to the lowest energies in a reliable fashion.

The most important exit channels in $^{12}C + ^{12}C$ fusion at low energies are ^{23}Na + p and $^{20}Ne + \alpha$ which populate discrete states in the final nuclei. The techniques used in the past to measure the fusion excitation function involved either charged-particle or γ-ray detection.

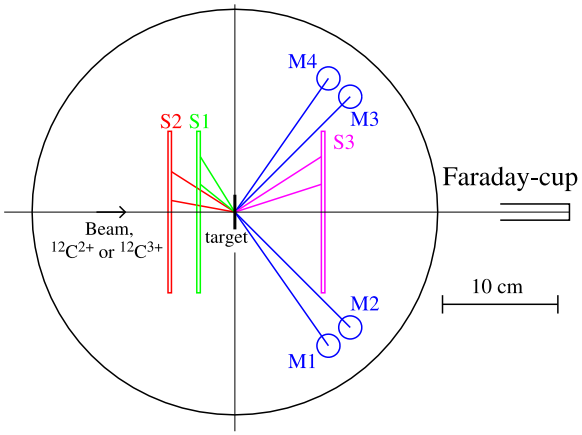

Figure 8. Experimental setup of the second experiment, using three DSSD's inside the Gammasphere target chamber. M are monitors. See text for details.

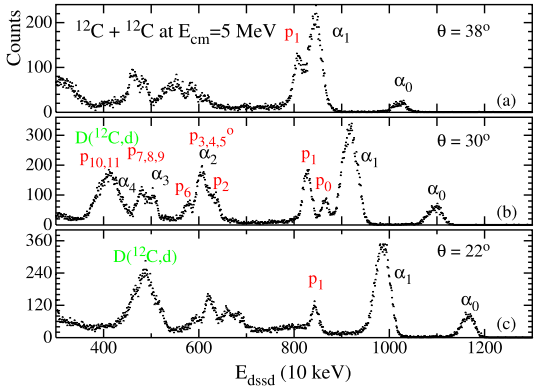

Figure 9. Single particle spectra from ring-1, 8 and 16 of the forward DSSD at E_{lab}=10 MeV. Ejectiles, α's (black) and protons (red) are indicated together with deuterons from the background reactions D(^{12}C,d).

In the charged-particle experiments, protons and α particles were detected with Si-detectors [5, 7, 30]. The detectors were usually covered by thin foils to absorb scattered ^{12}C particles. However, because of the ubiquitous hydrogen and deuterium contamination in the target, proton and deuteron recoil particles and d(^{12}C,p) reaction products can result in severe backgrounds at low beam energies.

Experiments based on γ-ray detection typically use large volume HPGe or Ge(Li) detectors [33, 31, 34, 16, 32, 9]. Most of these experiments detect the γ rays emitted from the first excited states of the evaporation residues ^{23}Na (0.440 MeV) or ^{20}Ne (1.634 MeV). Corrections for populating the ground states directly or for γ-ray transitions which do not pass through these first excited states, are usually taken from charged-particle measurements at higher energies. In these experiments, background events, originating from cosmic rays and from the environment can be suppressed by active or passive shielding. At very low bombarding energies, the γ-ray spectra also suffer from intense backgrounds at $E_\gamma = 2.36$ MeV and 3.09 MeV, originating from the H(^{12}C,γ)^{13}N and D(^{12}C,pγ)^{13}C reactions, respectively [31].

All previous measurements of ^{12}C + ^{12}C fusion excitation functions were performed in 'singles' mode. In this report, we discuss the advantages of measuring the charged particles in coincidence with γ rays from the decay of the evaporation residues, which leads to a considerable reduction of the background from target contaminants and from the environment. By using high-efficiency arrays of particle and γ-ray detectors, the associated reduction in detection efficiency can be compensated to a large extent.

In the present measurements, we used the Gammasphere detector at the ATLAS facility consisting of 101 Compton-suppressed Ge-detectors [35] to detect the γ rays from the evaporation residues ^{20}Ne and ^{23}Na . The light charged particles were detected in annular double sided Si-strip detectors (DSSD) of thickness 500 μm. Each detector was subdivided into 16 rings and 16 wedges. Two test experiments have been performed. 1) In the first experiment, only one DSSD was used covering the angular range θ = 22-39° when mounted in the forward hemisphere, or θ = 141-158° in the backward hemisphere, corresponding to a solid angle $\sim$ 7.4% of 4π. Alu-

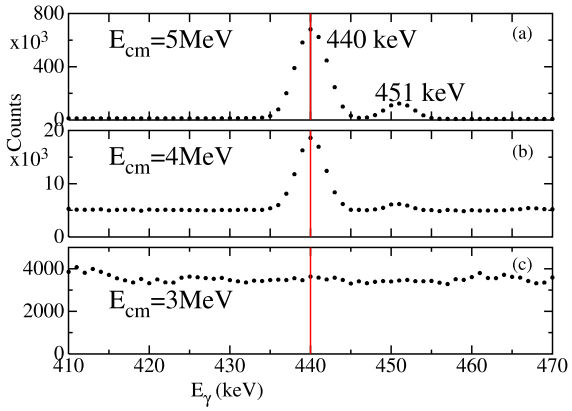

Figure 10. Single $\gamma-$ray spectra from Gammasphere at different incident energies. The 440-keV and 451-keV peaks are $\gamma-$ray transitions from ^{23}Na and ^{23}Mg, respectively.

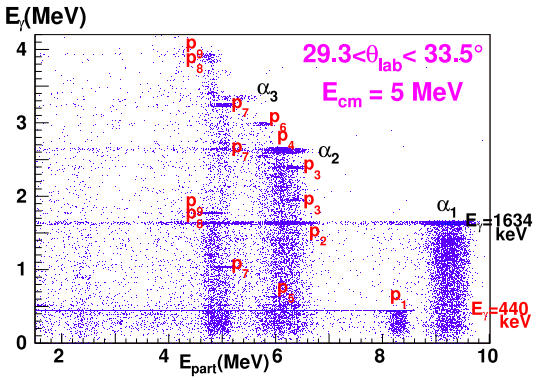

Figure 11. Two-dimensional coincidence spectrum of energy of γ rays vs. energy of particles integrated over four rings ($29.3° < \theta < 33.5°$).

minum foils with thicknesses of 10 μm at the forward or 1 μm at the back angles, respectively, covered the front of the DSSD, in order to absorb the elastically scattered ^{12}C particles and electrons from the target. Thin, isotopically enriched ($\geq$ 99.9% ^{12}C) and natural carbon targets with a thickness of about 40 μg/cm^2 were used. The measurements were performed at beam energies $E_{lab}(^{12}\mathrm{C}) = 10$, 9 and 8 MeV, with beam currents of 5-100 pnA. 2) In the second experiment, three DSSD's were installed as shown in Fig. 8, which covered the angular ranges of $17.7° < \theta < 32.6°$, $122.0° < \theta < 141.3°$ and $145.0° < \theta < 169.7°$, respectively. The total solid angle is about 20% of 4π. Aluminum foils with thicknesses of 28.4 mg/cm^2 for the forward or 0.35 mg/cm^2 for the backward DSSD's were used. Thin, isotopically enriched targets ($\geq$ 99.9% for ^{12}C and 99% for ^{13}C) with thicknesses of 40 μg/cm^2 and also an empty target were used. Most measurements were performed at beam energies of $E_{lab}(^{12}\mathrm{C}) = 10$, 9.6, 9.2, 8.6, 8 with a maximum beam intensity of 10 pnA. There was also a run at $E_{lab} = 6$ MeV with beam currents of only about 5 pnA, which also suppleid important results.

Three single-particle spectra from rings of the forward DSSD at $\theta_{lab} = 22$, 30 and 38° are shown in Fig. 9 at $E_{lab}(^{12}\mathrm{C}) = 10$ MeV. Different groups of protons and α's are indicated in Fig. 9. The change in energy with scattering angle reflects the kinematics, the energy losses in the target and the absorber foils. From these data angular distributions of protons and α's can be measured including the transitions to the ground states p_0, α_0, respectively. These spectra provide information about the ground state transitions, which cannot be detected by the γ-ray method. The transition p_0 to the ground state in ^{23}Na is hidden in the group α_1 at $\theta = 38°$. With the coincidence technique, these transitions can be measured separately.

The corresponding γ-ray single spectra from the decay of ^{23}Na obtained from the 101 Ge detectors in Gammasphere are found in Fig. 10 for $E_{lab} = 10$, 8 and 6 MeV, respectively. The spectra have been corrected for the Doppler shift of the outgoing ^{23}Na recoils. Slightly above the 440-keV transition in ^{23}Na, there is an additional weaker line at 451 keV, which corresponds to the $5/2^+ \rightarrow 3/2^+$ transition in ^{23}Mg, populated via the ^{12}C(^{12}C,n) reaction. Due to the Q values involved, this channel is closed at lower bombarding energies. At $E_{lab} = 10$ and 8 MeV the 440-keV transition is clearly visible. At $E_{lab} = 6$ MeV, however the 440-keV transition is hidden in the background because Gammasphere does not have good cosmic-ray shielding. The

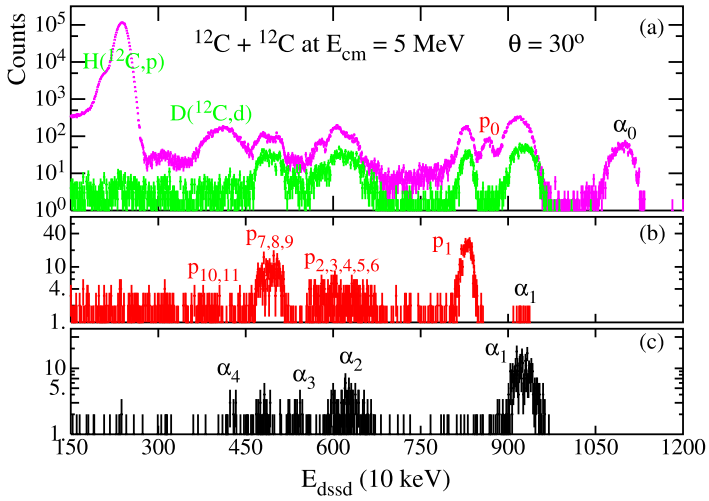

Figure 12. Particle-energy spectra detected at 30 ° and E_{cm} = 5 MeV. Magenta: without $\gamma-$ ray coincidence, green: coincidence with any γ rays, red: coincidence with E_γ = 440 keV, black: coincidence with E_γ = 1634 keV. The contaminations from the H(^{12}C,p) and D(^{12}C,d) reactions do not show up in the coincidence spectra.

background originating from the cosmic rays and the environment is relatively large. At E_{lab} = 6 MeV the fusion cross section of ^{12}C + ^{12}C is about 180 nb.

The background associated with 'singles' experiments can be removed if the charged particles and γ rays are measured in coincidence. This is seen from the two-dimensional plot of E_γ vs. E_{part} in Fig. 11. The various 'islands' associated with the population of states in ^{23}Na and ^{20}Ne are clearly separated. This is the case even for weak channels such as the decay of the 2^- state in ^{20}Ne at E_{ex} = 4.97 MeV, which decays via the 2^+ level at 1.63 MeV (marked α_3 in Fig. 11). Since the decay properties of excited states in the two residual nuclei are well known, the cross sections for producing the evaporation residues ^{23}Na and ^{20}Ne can be obtained. The spectrum shown in Fig. 11 was obtained in 30 minutes with a beam intensity of about 30 pnA.

In order to demonstrate the advantages of the coincidence technique, several particle-energy spectra are shown in Fig. 12, taken for one ring at 30° at E_{lab} = 10 MeV. The magenta spectrum does not require a $\gamma-$ray coincidence. The green spectrum is in coincidence with any γ-rays detected in the Gammasphere. In which, the contaminations from the H(^{12}C,p) and D(^{12}C,d) reactions do not show up. The red and black spectra are in coincidence with γ transitions E_γ = 440 or 1634 keV, respectively, corresponding to the proton channel (^{23}Na) and α channel (^{20}Ne). Because of Comptom scattering α_1 particles do show up in the proton spectrum, as well as protons in the α spectrum.

Based on these measurements it is now possible to estimate the count rates and background levels at even lower bombarding energies. It is clear that, in order to measure cross section in the 10 pb region, improvements in the detection efficiency as well as a considerable increase in beam intensity are needed. All results described above, except the γ-ray spectrum at E_{cm} = 3 MeV in Fig. 10, were obtained from the first test experiment with a single double-sided strip Si detector, mounted either at forward or backward angles covering a solid angle of 7.4% of 4π.

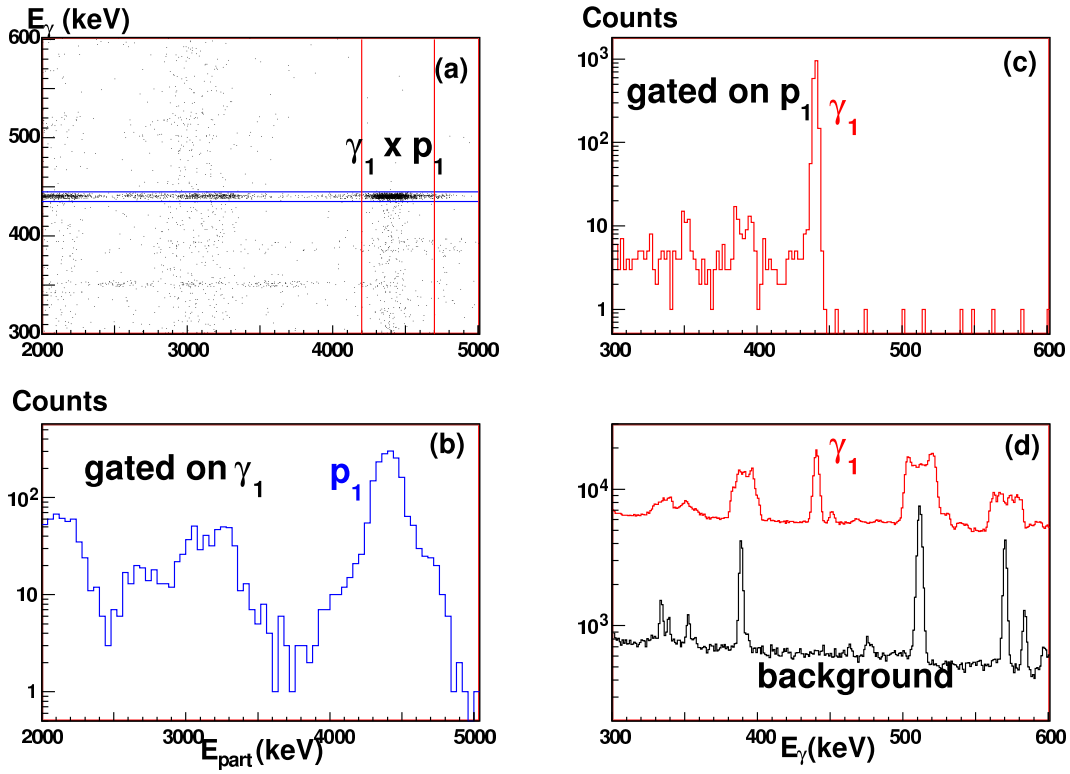

Figure 13. a): Two-dimensional spectrum E_γ versus E_{part} at E_{cm} = 4 MeV for the whole DSSD in the backward hemisphere. (b) and (c): Projections of events within the blue and red gates of (a) on the X-axis or the Y-axis, respectively. (d) Single E_γ spectra. See text for details.

This angle coverage can be increased to ∼20% as was done in the second experiment.

While higher beam currents are available from a variety of low-energy accelerators, the contributions from backgrounds, *e.g.* random coincidences need to be studied as well. For this purpose, the results obtained in the first experiment (using a higher beam intensity and longer running times at E_{lab} = 8 MeV) will be used. A part of the coincidence spectrum relevant for the population of the first excited state in ^{23}Na is given in Fig. 13(a) for the whole DSSD with two sets of gates corresponding to 435 keV < E_γ < 445 keV (blue) and 4.2 MeV < E_p < 4.7 MeV (red). The projection of Fig. 13(a), in coincidence with the γ-ray peak of E_γ = 440 keV is provided in Fig. 13(b) as a particle spectrum. Similarly, Fig. 13(c) is the projection of the events onto the γ-ray axis within the p_1 particle gate. In addition, two more γ-ray spectra are shown in Fig. 13(d): a single γ-ray spectrum taken at E_{cm} = 4 MeV (red) and a room-background spectrum measured during 2.5 hours without beam (black). Since the red spectrum has been corrected for the Doppler shift of ^{23}Na, the peaks from the room background are being transformed into broad groups. Inside the rectangle defined by the two set of gates in Fig. 13(a), there are about 1700 events, which were accumulated with a ^{12}C beam of 100 pnA in about 14 hours.

There are several kinds of backgrounds which can contribute to the coincidence counts : 1) random coincidence events between p_1 and the room background (including cosmic rays); 2) random coincidences between p_1 and Compton scattering of a higher-energy γ ray from another event; 3) reaction events from ^{12}C with a lower-mass target contaminant which appear inside the coincidence gates. From Fig. 13(d), the natural background rate of γ rays in the energy range of the coincidence gates is about 1 count/sec. In this test experiment the count rate in the particle detector at $E_{cm} = 4$ MeV within p_1 was about 0.33/sec and the rate of Compton scattering under the γ_1 peak at 435 - 455 keV was < 1/sec. Thus, with a (conservative) coincidence time window of 1 μs, the random coincidence backgrounds of 1) and 2) are each of the order of 5×10^{-7}/sec. This needs to be compared with the γ_1 - p_1 coincidence rate of about 0.034/sec, resulting in a background/signal ratio of 3×10^{-5}.

For a measurement at very low energies, the beam intensity needs to be increased by a factor of $\sim$ 1000. The effect of this increase in beam intensity on the count rate is difficult to predict since it depends on the details of the experimental setup and on the divergence of the beam. Scattering from collimators and the Faraday cup did not contribute in this test experiment due to the low energy of the incident ^{12}C particles. At a bombarding energy of $E_{lab} = 8$ MeV the total count rate in the $\sim$100 Ge detectors of Gammasphere increased by about only 1% with and without beam. This increase in count rate is expected to be even less at lower energies where increases in beam intensity are needed. Precise numbers, however, can only be obtained from a real experiment. The detector count rate is not expected to increase proportionally to beam intensity as the beam energy is reduced since all cross sections producing particle and γ-rays fall off precipitously with energy. But even if we use the background/signal ratio mentioned above (3×10^{-5}) as a reference, it can increase by a factor of 500 before reaching a value of about 1.5%. The background from lower-mass target contaminants may increase at the lowest energies. However, because the two gates for the charged particles and γ rays are well defined, and since the reaction products from the lighter target contaminants are well known, one should be able to identify and reject this background. A detailed analysis, however, requires a full experiment. With a γ_1 - p_1 coincidence rate of about 2/day (beam current 100 pμA) one should be able to reach cross sections of 10 pb with rather low background. This is a conservative estimate by only using γ_1 - p_1 coincidences. In practice, other coincidences events can be used as well.

Another issue that needs to be addressed is the choice of the target for experiments with beam intensities between 10-100 pμA. If a thin rotating carbon target can not withstand the high beam currents, a thick water-cooled target [9] can be used. This choice has the additional advantage that the contribution from light-particle contaminants will be strongly reduced due to the heating of the target material. A disadvantage is the reduction in solid angle for particle detection by a factor of $\sim$ 2 as compared to the last estimate, since only particles emitted in the backward hemisphere can be detected. The expected γ_1 - p_1 coincidence rate is, then about 2 counts/day for cross sections of 20 pb.

The aim of the second experiment was to test some of the estimates mentioned above. Unfortunately, the ion-source of the tandem during that experiment, provided only 5 - 10 pnA of ^{12}C beam. However, a measurement for 10 hours with about 5 pnA at $E_{lab} = 3$ MeV was performed, and the result is shown in Fig. 14 and 15. In Fig. 14(a) we show plots similar to these of Fig. 13. These are spectra for three DSSD's all together. Inside the two gates : γ_1 and p_1, one good event has been observed. No coincidence-background events were detected in a rather large region surrounding this event. Random coincidence events appear only at low energies of E_{DSSD}, In Fig. 14(b) and (c), the blue count is the projection from this good event. The green

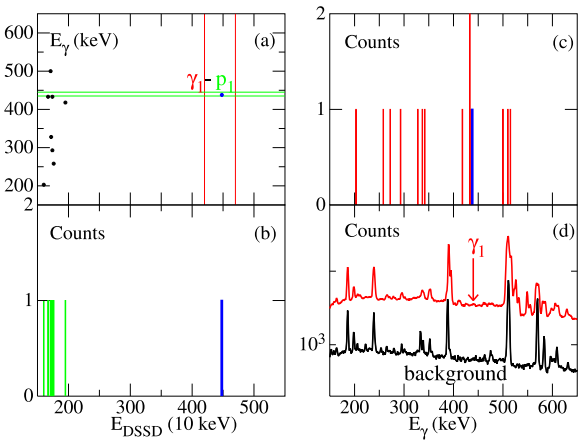

Figure 14. (a): Two-dimensional spectrum E_γ versus E_{part} at E_{cm} = 3 MeV. Projection of one event within the green and red gates of (a) on the X-axis or the Y-axis, respectively, are shown by the blue one in (b) and (c). The green in (b) and red in (c) are projections of events in (a) on the X-axis or the Y-axis, respectively. (d): Single E_γ spectra. See text for details.

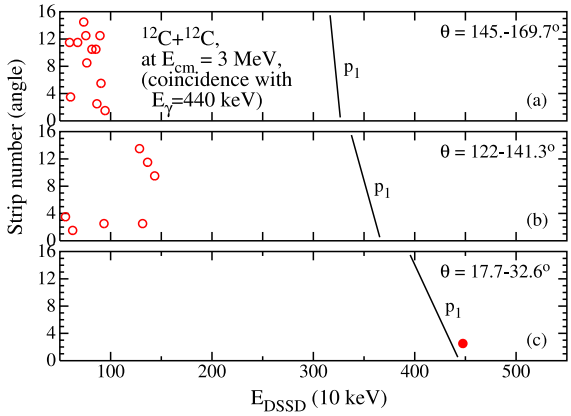

Figure 15. Coincidence spectra for the three DSSD's separately at E_{cm} = 3 MeV, gated with a γ-ray of 435 keV $< E_\gamma <$ 445 keV. The solid circle is the only one good event observed, corresponding to the blue one in Fig. 14. The open circles are backgrounds. See text for details.

and red counts in Fig. 14(b) and (c) are the total projections (without gates) from (a). Another plot, for the particle spectra of three DSSD's separately, is shown in Fig. 15. They are gated with a γ-ray of 435 keV $< E_\gamma <$ 445 keV for the same run as Fig. 14. Three lines indicate the expected energies for the most important and strongest particle group p_1. Obviously the only one good coincidence event locates at the right energy. There are background events, red open circles show up at low E_{DSSD} in Fig. 15(a) and (b). These are due to the random coincidence between low energy counts in DSSD's and $\gamma-$ray background. In fact, we did find that the beam-collimator system in this experiment was not very good. A very small amount of beam particles did hit on the two backward DSSD's directly through the multiple-scattering processes inside the beam line. These backgrounds can be prevented easily in a setup with better collimators.

The cross section obtained from this one good event during this ten-hours run does agree with the value estimated from the previous experiments within the uncertainty. The observed background situation also supplied us a positive check about the discussion given above.

The experimental result has shown that a particle-γ coincidence technique provides very clean spectra. The contributions from populating the ground states in ^{20}Ne and ^{23}Na can be obtained from the singles spectra of the DSSD's at higher energies. Based on these test results, it appears possible to measure the fusion cross section of the astrophysically important ^{12}C + ^{12}C reaction down to the 10 pb level, if beam currents of the order of 100 pμA and sufficiently long running times ($\sim$10 days) are available. It is an expectation, and should be checked in real measurements in the future.

Although the Gammasphere array is unique, similar arrays consisting of several clover detectors can be constructed with comparable detection efficiency. For example five HPGe clover

detectors (four centered at 90° with respect to the beam axis and one placed at 0°) will have a photopeak efficiency of $\sim 20\%$ as demonstrated *e.g.* in the X-array at ATLAS. The particle-γ coincidence efficiency of such an arrangement is $\sim 6\%$, *i.e.* similar to that achieved in 'singles' γ-ray measurement [9]. This will allow for improved measurements of this important reaction at very low energies. The particle-γ technique can also be applied to studies of other systems where background reactions in singles experiments limit the extraction of the cross sections, such as in the fusion reactions ^{12}C + ^{16}O and ^{16}O + ^{16}O. Some of the experimental results of the first experiment have been published in Ref. [36].

4. Acknowledgements

This work was supported by the US Department of Energy, Office of Nuclear Physics, under Contract No. DE-AC02-06CH11357 and by the NSF under Grant No. PHY-0758100 and PHY-0822648. The authors want to thank M. Hussein, R. Charity and A. Karpov for valuable discussions.

References

[1] Rolfs C E and Rodney W S, Cauldrons in the Cosmos (The University of Chicago press, Chicago, 1988)
[2] Fowler W, Caughlan G and Zimmerman B 1975 Annu. Rev. Astrophys. **13** 69
[3] Barnes C A, Trentalange S and Wu S C 1985 Treatise on Heavy-ion Science, edited by D.A. Bromley, Vol. 6, page 3, (Plenum, New York 1985)
[4] Gasques L R *et al.* 2005 Phys. Rev. **C 72** 025806
[5] Patterson L J, Winkler H, and Zaidins C S 1969 As. J. **157** 367
[6] Kovar D *et al* 1979 Phys. Rev. **C 20** 1305
[7] Becker H W, Kettner K U, Rolfs C, and Trautvetter H P 1981 Z. Phys. **A 303** 305
[8] Satkowiak L J *et al.* 1982 Phys. Rev. **C 26** 2027
[9] Spillane T *et al.* 2007 Phys. Rev. Lett. **98** 122501
[10] Jiang C L *et al.* 2007 Phys. Rev. **C 75** 015803
[11] Jiang C L *et al.* 2002 Phys. Rev. Lett. **89** 052701; 2004 Phys. Rev. Lett. **93** 012701
[12] Mişicu Ş and Esbensen H 2006 Phys. Rev. Lett. **96** 112701; 2007 Phys. Rev. **C 75** 034606
[13] Almqvist E, Bromley D A, and Kuehner J A 1960 Phys. Rev. Lett. **4** 515
[14] Erb K A *et al.* 1980 Phys. Rev. **C 22** 507
[15] Christensen P R and Switkowski Z E 1977 Nucl. Phys. **A 280** 205
[16] Aguilera E F *et al.* 2006 Phys. Rev. **C 73** 064601
[17] Krappe H J, Nix J R, and Sierk A J 1979 Phys. Rev. **C 20** 992
[18] Esbensen H, Tang X D, and Jiang C L 2011 Phys. Rev. **C 84** 064613
[19] Dayras R A*et al.* 1976 Nucl. Phys. **A 285** 153
[20] Notani M *et al.* 2012 Phys. Rev. **C 85** 014607
[21] Trentalange S *et al.* 1988 Nucl. Phys. **A 483,** 406
[22] Charvet J L *et al.* 1982 Nucl. Phys. **A 376** 292
[23] Vandenbosch R 1979 Phys. Lett. **B 87** 183
[24] Iljinov A S *et al.* 1992 Nucl. Phys. **A 543** 517
[25] Beckerman M 1978 Nucl Phys. **A 278** 333
[26] http://www.nndc.bnl.gov/nudat2/adopted-searchi.isp
[27] Moldauer P A, 1967 Phys. Rev. **157** 17
[28] Jiang C L *et al.* 2006 Phys. Rev. **C 73** 014613
[29] Zickefoose J 2011 Thesis, U. Conn.; or see www.lsw.uni-heidelberg.de/nic2010/talks/Strieder.pdf
[30] Mazarakis M *et al.* 1973 Phys. Rev. **C 7** 1280
[31] Kettner K U *et al.* 1980 Z. Phys. **A 298** 65; 1977 Phys. Rev. Lett. **38** 337.
[32] Barron-Palos L R *et al.* 2006 Nucl. Phys. **A 779** 318
[33] Dasmahapatra B *et al.*, 1982 Nucl. Phys. **A 384** 257
[34] Rosales P *et al.* 2003 Rev. Mex. Fís. **49** (S4) 88
[35] Lee I Y 1990 Nucl. Phys. **A 520** 641c
[36] Jiang C L *et al.* 2012 Nucl. Inst. Meth. **A 682** 12